An Adaptive Digital Method of Imbalances Cancellation in LINC Transmitters

Paloma García, Jesús de Mingo, *Member, IEEE*, Antonio Valdovinos, and Alfonso Ortega

***Abstract*—The linear amplification using nonlinear components (LINC) technique is a well-known power amplifier linearization method to reduce adjacent channel interference in a nonconstant envelope modulation system. Its major drawback is the inherent sensitivity to gain and phase imbalances between the two amplifier branches. In this paper, a novel full-digital base band method is described which corrects any gain and phase imbalances in LINC transmitters mainly due to the unmatching of the two amplifier paths. Amplifiers are characterized by a level-dependent complex gain using a memoryless model. The method uses adaptive signal processing techniques to obtain the optimal complex coefficient to adjust gain and phase imbalances. Its main advantage is the ability to track the input signal variations and adapt to the changes of amplifier nonlinear characteristics. Other effects are included in the analysis such as quadrature modulator and demodulator imbalances and loop delay. A computer simulation has been carried out to verify the method functionality.**

***Index Terms*—Adaptive digital method, amplifier linearization, imbalances correction, LINC transmitter.**

I. Introduction

THE growing demand for mobile communications services and the limit of the frequency spectrum have increased the use of spectrally efficient modulations, most of which have nonconstant envelopes. As a result of transmitter nonlinearities (mainly from the power amplifier), the transmitted signal spectrum expands into adjacent channels, an effect known as adjacent channel interference (ACI). Some systems, such as terrestrial trunked radio (TETRA), are very restrictive with regard to spurious emission in the adjacent channel. In the TETRA system, the spurious emission in the first adjacent channel must be less than −60 dBc. One way to achieve linear amplification is by using a class A power amplifier well below saturation with an appropriate backoff. However, this implies low power efficiency, which is unsuitable for equipment with restrictive battery capacity requirements. High power efficiency can be obtained with class AB, B, or C power amplifiers but they are more nonlinear. In order to achieve both spectrum and power efficiency, several classical linearizing techniques for power amplifiers have been proposed in the technical literature. These techniques are usually categorized as feed-forward, feedback, predistortion and linear amplification with nonlinear components (LINC) transmitter. A LINC transmitter (see Fig. 1) presents some drawbacks. One of them is that most of the radio-frequency power is in the distortion signal, which is cancelled in the combiner; thus applications with large peak to average power ratio experience a significant loss in power efficiency. Several studies about this issue can be found in [19]–[23]. Another one is its inherited sensitivity to gain and phase imbalances between the two amplifier branches [1], [2]. Several authors have considered methods to correct the imbalances in LINC transmitters [3]–[7], but the novel method presented here uses adaptive signal-processing techniques. It is carried out in baseband and is full-digital.

Manuscript received June 5, 2003; revised January 21, 2004; November 25, 2004. This work was supported by the Spanish Ministry of Science and Technology and FEDER under Projects CICYT TEC2004-04529 and TIC2001-2481. The review of this paper was coordinated by Prof. T. Lok.

The authors are with the Electronics Engineering and Communications Department, University of Zaragoza, Zaragoza E-50018, Spain.

Digital Object Identifier 10.1109/TVT.2005.844641

II. Imbalance Effects in a LINC Transmitter

One of the reasons that the LINC transmitter has not been widely used is the difficulty to achieve the accurate gain and phase matching required between the two paths. Errors in gain and/or phase matching cause incomplete cancellation of unwanted elements in wide-band phase modulated signals. As a result, a large number of unwanted spurious products appear in the output spectrum, as observed previously [1], [2], [4], [11].

The effect of gain and phase imbalances between the two paths may be analyzed as follows. The source signal may be written in complex general format as [11]

$$s(t) = c(t)e^{j\rho(t)} \quad 0 < c(t) \leq c_{\max}. \tag{1}$$

The source signal is separated into two constant-envelope signals by a signal component separator (SCS) as shown in Fig. 1. These signals are calculated as

$$\begin{aligned} s_1(t) &= \frac{s(t)}{2}\left[1 - e_s(t)\right] \\ s_2(t) &= \frac{s(t)}{2}\left[1 + e_s(t)\right] \end{aligned} \tag{2}$$

where $e_s(t)$ is a signal that is in quadrature to the source signal $s(t)$.

$$e_s(t) = j\sqrt{\left[\frac{c_{\max}^2}{|s(t)|^2} - 1\right]}. \tag{3}$$

Thus

$$s(t) = s_1(t) + s_2(t) \quad \text{and} \quad |s_1(t)| = |s_2(t)|. \tag{4}$$

The amplifier of each path is characterized by a level-dependent complex gain, with an output signal in each path given by

$$s_{o1}(t) = v_1(t) \cdot G_1\left(|v_1(t)|\right) \quad s_{o2}(t) = v_2(t) \cdot G_2\left(|v_2(t)|\right) \tag{5}$$

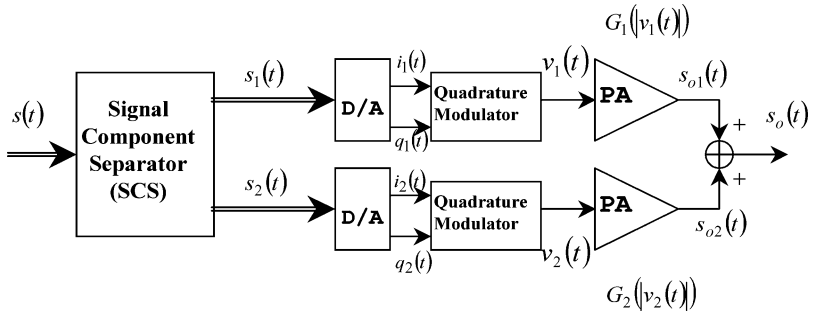

Fig. 1. Schematic diagram of the LINC transmitter.

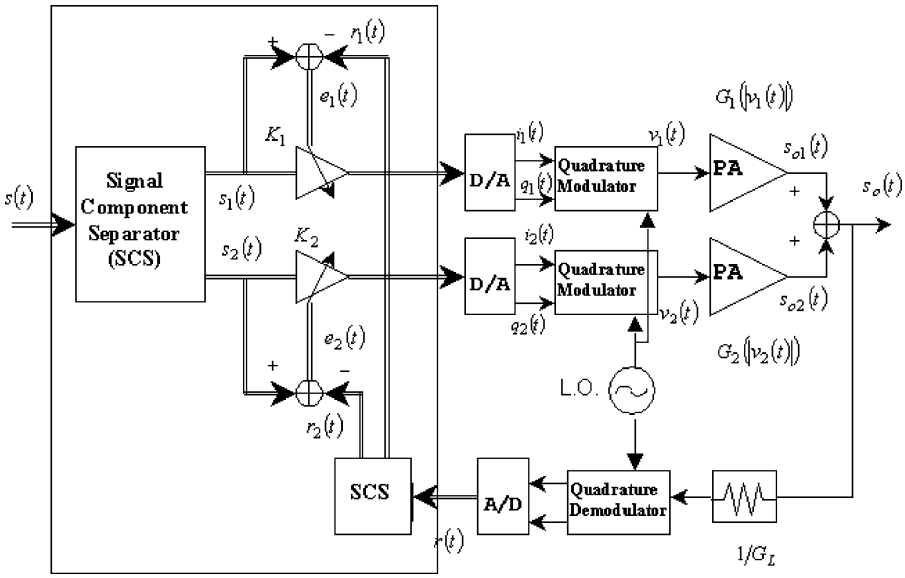

Fig. 2. Simulation model of the correction method.

where $v_1(t)$ and $v_2(t)$ are the complex baseband representation of the instantaneous input complex modulation envelope of the power amplifier in each path. Therefore, if ideal digital-to-analog converters (DACs) and quadrature modulators are supposed, that is, $s_1(t) = v_1(t)$ and $s_2(t) = v_2(t)$, the output signal in complex format then becomes

$$\begin{aligned} s_o(t) &= s_{o1}(t) + s_{o2}(t) \\ &= s_1(t) \cdot G_1(|v_1(t)|) + s_2(t) \cdot G_2(|v_2(t)|) \\ &= s(t) \cdot \frac{G_1(|v_1(t)|) + G_2(|v_2(t)|)}{2} \\ &\quad - s(t) \cdot e_s(t) \cdot \frac{G_1(|v_1(t)|) - G_2(|v_2(t)|)}{2}. \end{aligned} \quad (6)$$

The second term in (6) implies that there is an unwanted residual signal due to imperfect cancellation (it tends to zero as the gain and phase matching are perfected). The term introduces interfering power in the adjacent channel limiting the spectrum efficiency of the system. The aim of this method is to reduce factor $[G_1(|v_1(t)|) - G_2(|v_2(t)|)]$ as much as possible. The method is based on adaptive signal processing techniques, and its main advantage is to track input signal variations and possible changes due to temperature variations and component aging, among others.

III. Model of the Correction Method

A schematic diagram of the simulation model of this correction method is depicted in Fig. 2. The source signal is separated into the two constant-envelope signals by a signal component separator (SCS) block. These signals are multiplied by different complex coefficients, one for each branch (K_1 and K_2). The coefficients are computed to reduce the adjacent channel interference by means of an adaptive algorithm. This algorithm needs a reference of the output signal to update the complex coefficients. A reference signal $r(t)$ is obtained by means of a down-conversion process of the output signal $s_o(t)$ applying a down-conversion gain $1/G_L$, which is calculated to adjust the range of values to the quadrature demodulator input. This reference signal can be split into two signals using an SCS block to obtain the two error signals (one for each path), needed for the adaptive algorithm. A common oscillator for the quadrature modulators and demodulator is used. The phase shifts of the oscillator signal between different modulators and demodulator will not be a problem because they are absorbed in the adaptation of complex coefficients K_1 and K_2.

The adaptation criterion of the algorithm is to minimize the mean squared error in each path. The error signal for each path is defined as

$$e_1(t) = s_1(t) - r_1(t) \qquad e_2(t) = s_2(t) - r_2(t) \quad (7)$$

where $r_1(t)$ and $r_2(t)$ are obtained from $r(t)$ using a signal component separator block

$$r_1(t) = \frac{r(t)}{2}\left[1 - e_r(t)\right]$$
$$r_2(t) = \frac{r(t)}{2}\left[1 + e_r(t)\right]. \tag{8}$$

Assuming ideal DACs, analog-to-digital converter (ADC), and quadrature modulators and demodulator, the reference signal $r(t)$ is

$$\begin{aligned} r(t) &= r_1(t) + r_2(t) \\ &= \frac{s_o(t)}{G_L} \\ &= \frac{s_1(t)K_1G_1\left(|v_1(t)|\right) + s_2(t)K_2G_2\left(|v_2(t)|\right)}{G_L}. \end{aligned} \tag{9}$$

Similarly to (1), the signal $r(t)$ can be written in complex general format as

$$r(t) = z(t)e^{j\alpha(t)} \qquad 0 < z(t) \le z_{\max} \tag{10}$$

and $e_r(t)$ is computed as

$$e_r(t) = j\sqrt{\left[\frac{z_{\max}^2}{|r(t)|^2} - 1\right]}. \tag{11}$$

The cost functions to minimize are defined as

$$J_1 = E\left[|e_1(t)|^2\right] \quad J_2 = E\left[|e_2(t)|^2\right] \tag{12}$$

where $E[.]$ denotes the statistical expectation operator.

In following formulas, $G_1(|v_1(t)|)$ and $G_2(|v_2|(t)|)$ will be denoted as G_1 and G_2 to simplify terms.

The gradient of the cost function is calculated by means of the partial derivatives with respect to Kr_n and Ki_n and can be written as

$$\nabla_{K_n} J_n = \frac{\partial J_n}{\partial Kr_n} + j\frac{\partial J_n}{\partial Ki_n} \quad n = 1, 2 \tag{13}$$

with $K_n = Kr_n + jKi_n$ and where Kr_n denotes the real part and Ki_n the imaginary part of K_n.

For the cost function J_n to attain its minimum value, all the terms of the gradient must be simultaneously equal to zero.

Computing the cost function (12) gives

$$\begin{aligned} J_n &= E\left[e_n(t) \cdot e_n(t)^*\right] \\ &= E\left[\left(s_n(t) - r_n(t)\right) \cdot \left(s_n(t) - r_n(t)\right)^*\right] \\ &= E\left[|s_n(t)|^2 + |r_n(t)|^2 - s_n(t)r_n^*(t) - s_n^*(t)r_n(t)\right] \\ &\quad n = 1, 2. \end{aligned} \tag{14}$$

Assuming the following approximation, which is valid for the source signal proposed in the next section:

$$r_n(t) \approx \frac{s_n(t)K_nG_n}{G_L} \quad n = 1, 2. \tag{15}$$

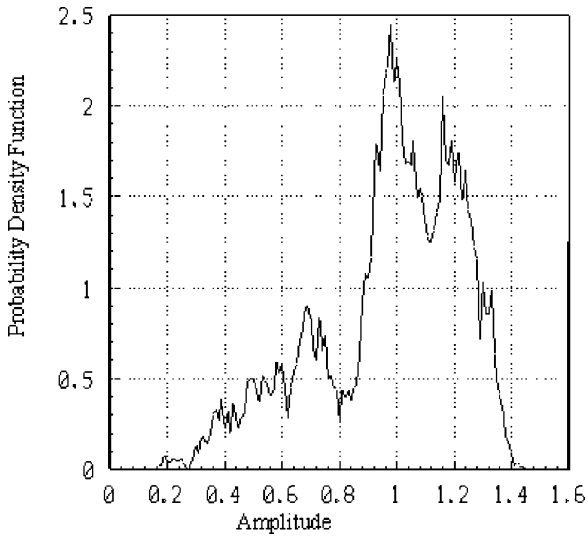

Fig. 3. Probability density function with respect to the envelope of a TETRA signal.

The gradient of the cost function for each path defined by (12) gives

$$\begin{aligned} \nabla_{k_n} J_n \approx &-2 \cdot E\left[|s_n(t)|^2 \right. \\ &\cdot \left(\frac{K_n|G_n|^2}{|G_L|^2} - \frac{G_n^*}{G_L^*} \right. \\ &\left. \left. + \frac{|K_n|^2 \frac{\partial |G_n|^2}{\partial K_n^*}}{|G_L|^2} - \frac{K_n^* \frac{\partial G_n^*}{\partial K_n^*}}{G_L^*} - \frac{K_n \frac{\partial G_n}{\partial K_n^*}}{G_L} \right) \right] \\ &n = 1, 2. \end{aligned} \tag{16}$$

The partial derivative terms of the gain G_n respect to the variable K_n are very close to zero in the working region of the amplifier. Finally, making this approximation and applying (7), (17) is obtained for each path

$$\nabla_{k_n} J_n \approx -2 \cdot E\left(e_n(t) \cdot \left(\frac{r_n(t)}{K_n}\right)^*\right) \quad n = 1, 2. \tag{17}$$

Therefore, using the instantaneous estimate of the gradient, the updated value of the adaptive coefficient at time $\mathrm{m}+1$ is computed by using the simple recursive relation

$$K_n(m+1) = K_n(m) + \mu_n \cdot e_n(m) \cdot \left(\frac{r_n(m)}{K_n(m)}\right)^* \quad n = 1, 2 \tag{18}$$

where the positive real-valued constant μ_n (step-size), controls the speed of convergence and the algorithm misadjustment (final excess error).

The made approximations will produce a residual error in the proposed architecture performance. Although a residual error appears, if the proposed model gets a reduction of the out-of-band interference respect to the single amplifier model, the presented architecture could be validated. The research, by means of simulations, of the proposed correction method applying the adaptive algorithm given by (18) is presented in the next section.

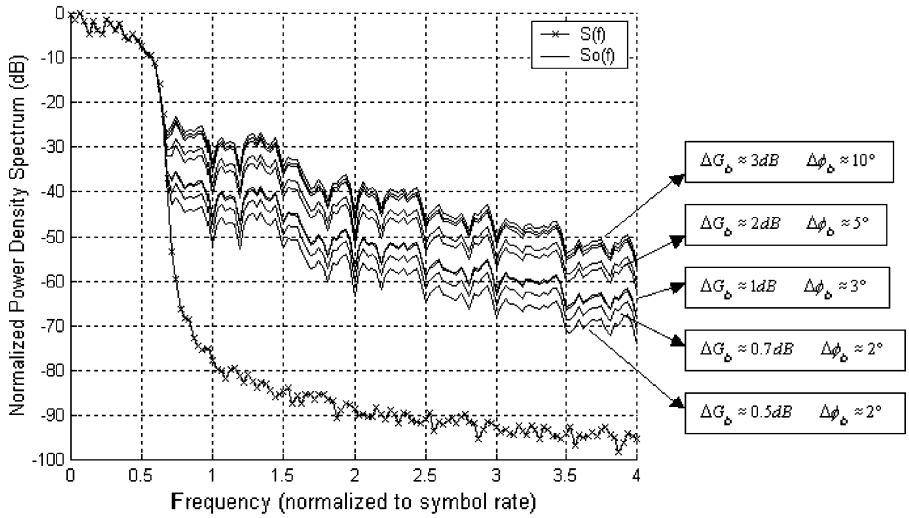

Fig. 4. Normalized power density spectrum of simulated input $S(f)$ and output $S_o(f)$ with several gain and phase imbalances in the second branch of a LINC transmitter without correction method.

IV. Simulations

The source signal for simulations is a $\pi/4$ differential quaternary phase-shift keying modulated signal filtered with a squared-root raised cosine with a 0.35 rolloff factor at 36 Kbps, which corresponds to a TETRA signal. The envelope value range of a TETRA signal is shown in Fig. 3, including the probability density function with respect to the modulated signal envelope for a sequence of 8200 symbols (with eight samples per symbol).

The amplifier is characterized by a complex gain using a memoryless model, which depends on the input signal level. A common method to model power amplifiers taking into account nonlinearities with memory is to use a Volterra series representation. For most amplifiers, where the modulation bandwidth is much less than the carrier frequency, the memory in the nonlinearity is small enough to be neglected, and the Volterra series can be simplified into a simple power series with complex coefficients, as shown in successful implementations [9], [10], [17], [25] and studies [18], [24]. The complex gain of the amplifier is extracted from measurements of AM–AM and AM–PM conversion of a Mitsubishi M68749 amplifier (with a driver) at 390 MHz (50 Ω system) [12]. A polynomial regression is used to model the amplifier complex gain of each path

$$G_n\left(|v(t)|\right) = M_n\left(|v(t)|\right) \cdot e^{j\Phi_n(|v(t)|)} \quad n = 1,2 \tag{19}$$

$$\begin{aligned} M_n\left(|v(t)|\right) = {} & 200\alpha_{n,1} + 800\alpha_{n,2}\,|v(t)| - 12\,760\alpha_{n,3}\,|v(t)|^2 \\ & + 67\,930\alpha_{n,4}\,|v(t)|^3 - 193\,540\alpha_{n,5}\,|v(t)|^4 \\ & + 281\,970\alpha_{n,6}\,|v(t)|^5 - 162\,240\alpha_{n,7}\,|v(t)|^6 \end{aligned} \tag{20}$$

$$\begin{aligned} \Phi_n\left(|v(t)|\right) = {} & 1.1426\beta_{n,1} + 2.2584\beta_{n,2}\,|v(t)| \\ & - 27.676\beta_{n,3}\,|v(t)|^2 + 147.2407\beta_{n,4}\,|v(t)|^3 \\ & - 461.0754\beta_{n,5}\,|v(t)|^4 + 722.6528\beta_{n,6}\,|v(t)|^5 \\ & - 432.1345\beta_{n,7}\,|v(t)|^6 . \end{aligned} \tag{21}$$

The amplifier in path 1 is simulated with

$$\alpha_{1,j} = 1 \qquad \beta_{1,j} = 1 \qquad j = 1 \ldots 7.$$

The amplifier in path 2 is simulated introducing several imbalances in some coefficients of the gain and phase polynomial. Several tests have been carried out by modifying the factors $\alpha_{2,j}$ and $\beta_{2,j}$ around $\pm 10\%$.

It has to be said that the frequency response of both amplifiers and the combiner has been considered flat across a band frequency roughly 200 KHz (up to the fourth adjacent channel), which can be achieved in practice. If this does not occur, the presented architecture will not work properly for the proposed modulated source signal.

The downconversion gain has been simulated as an estimation of the reverse of the total equivalent linear gain of the power amplifier.

Fig. 4 shows the normalized input $S(f)$ and output $S_o(f)$ power density spectrum for a 3-W output power amplifier under different gain (ΔG_b) and phase imbalances $(\Delta\phi_b)$ between both branches of the LINC transmitter (without applying the correction method). This figure illustrates the effect of gain and phase imbalances and the need for a method to achieve gain and phase matching as presented in this paper.

Fig. 5 compares the normalized input and output power density spectrum with and without the presented adaptive correction method and with a gain imbalance of approximately 1.5 dB and a phase imbalance around 5° between two amplifying branches (an ideal feedback branch is assumed). As seen in Fig. 5, the ACI is improved after applying the correction method with accurate gain and phase matching between the two paths. The ACI in the first adjacent channel without correction is around -35 dBc, but below -64 dBc using the correction method ($\approx$30 dB improvement).

Using this method, the speed of convergence can be measured by analyzing the time evolution of error signals $e_1(t)$ and $e_2(t)$. The step size parameter μ_n was chosen to reduce the ACI (up to -60 dBc in the first adjacent channel) as quickly as possible. The convergence time has to be smaller than 6.6 ms, which is the reserved time in TETRA for the linearization slot. As seen in Fig. 6, the convergence time ($< 1\ \mu$s) is suitable in order to be implemented in a real system.

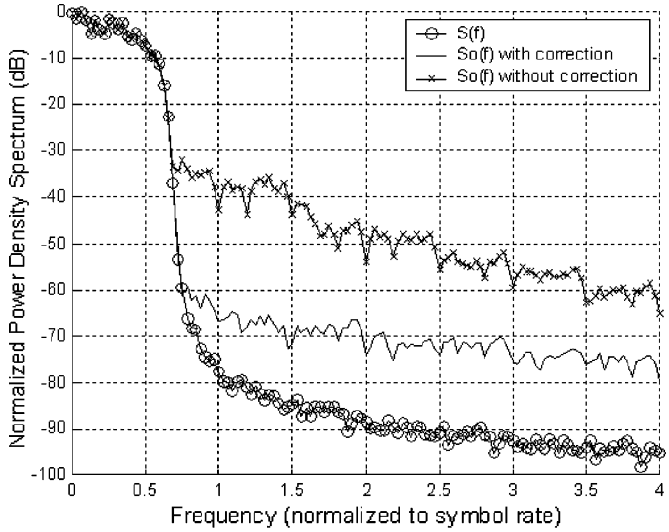

Fig. 5. Normalized power density spectrum of simulated input $S(f)$ and output $S_o(f)$ with and without applying the proposed correction method.

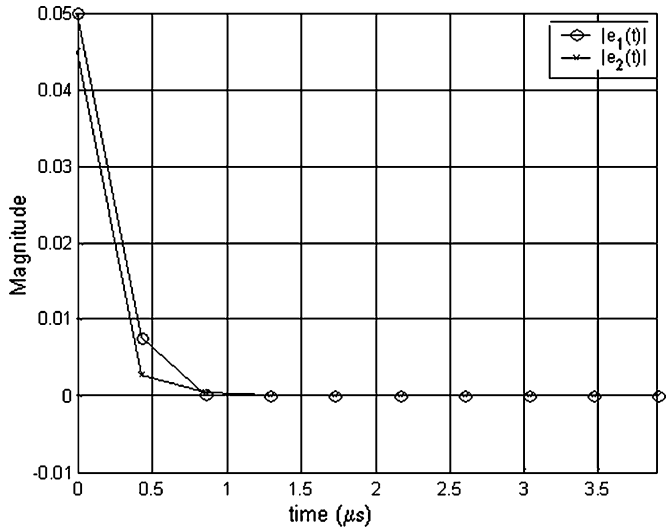

Fig. 6. Evolution of error signals in each path.

As mentioned above, the downconversion gain is simulated as an estimation of the reverse of total equivalent linear gain of the power amplifier. We now consider how an error in the estimation of the downconversion gain influences on the method performance. Simulations have been carried out varying the value of the downconversion gain by ± 0.3 dB in amplitude and $\pm 5^\circ$ in phase. The downconversion gain value has to be appropriate in order to compare signals $s_n(t)$ with $r_n(t)$ correctly. Fig. 7 shows that an error in the estimation of the downconversion gain has little influence on the performance of this correction method.

A. Modulator and Demodulator Misalignments

Perfectly balanced quadrature modulators and demodulator have been assumed in this architecture in previous sections, which leads to another practical consideration. The quadrature imbalances (amplitude and phase) create a residue in the adjacent channel, increasing the ACI [13], [14]. Fig. 8 shows the degradation of the ACI when there are imbalances in the quadrature modulators. Simulations have been carried out with several amplitude and phase imbalances, which can be seen in Fig. 8. We present in Fig. 9 the results, based on simulations, that show the influence of the amplitude and phase imbalances of the quadrature modulator in the proposed architecture on the ACI measurement in the first adjacent channel (25 KHz) in the TETRA standard. The results are very promising for imbalance values corresponding to commercial quadrature modulators (amplitude error between 0.5 and 1 dB and phase error between 2° and 5°).

In the same way, in the feedback branch, the effect of an unbalanced quadrature demodulator in this architecture has been analyzed. Some simulations have been carried out with gain and phase errors of commercial quadrature downconverters. Fig. 10 shows the influence of phase and amplitude imbalances of the I/Q demodulator on the ACI measurement (in the first adjacent channel). It can be seen that the effect of the quadrature downconverter imbalances (gain and phase) on the overall system performance is not very significant.

We have considered two identical unbalanced quadrature modulators in each path, but in the worst case each I/Q modulator could have different amplitude and phase errors. Fig. 11 includes several simulations with different gain and phase imbalances values in the I/Q modulator of each path and in the I/Q demodulator. The Adjacent Channel Interference under real conditions increases but the TETRA requirement regarding the ACI is met. Table I shows the simulated imbalances in both quadrature modulators and the demodulator and the resulting ACI value in each simulation.

B. Imbalance Effects on the Vector Error

The vector error is another important requirement in transmission in digital communication systems. The vector error has to be less than 10% for the TETRA standard. The effects of the gain and phase imbalances on the vector error may be analyzed as follows [15]:

$$Ev = \sqrt{(R^2 + M^2) - 2RM\cos(\alpha_e)} \tag{22}$$

where R is the magnitude of the "ideal'" vector (the unity in the TETRA modulation), M is the magnitude of the measured vector, and α_e is the phase error between them. The measured vector magnitude M is composed of the "ideal" magnitude R plus a component resulting from the gain error present in the system G_e. Therefore, (22) can be written as

$$Ev = \sqrt{(1 + (1 + G_e)^2) - 2(1 + G_e)\cos(\alpha_e)}. \tag{23}$$

The received signal constellation without and with the correction method is shown in Fig. 12(a) and (b), respectively. An expanded point of the previously received signal constellation is presented in Fig. 12(c) and Fig. 12(d) for a better comparison of the vector error. Thus, the vector error improves after the correction method is applied, obtaining a residual vector error less than 10%, so the TETRA requirement is met in terms of vector error.

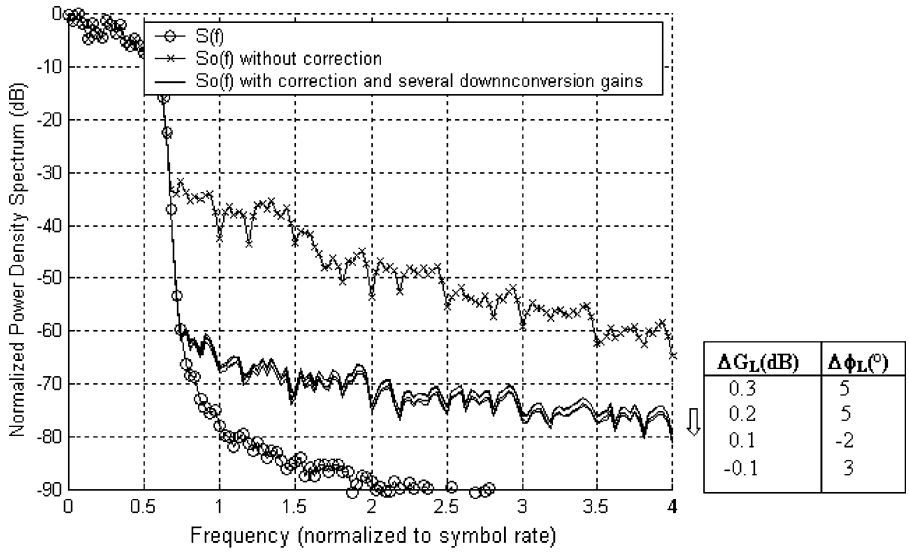

Fig. 7. Normalized power density spectrum of simulated input $S(f)$ and output $S_o(f)$ with different errors in the estimation of the downconversion gain.

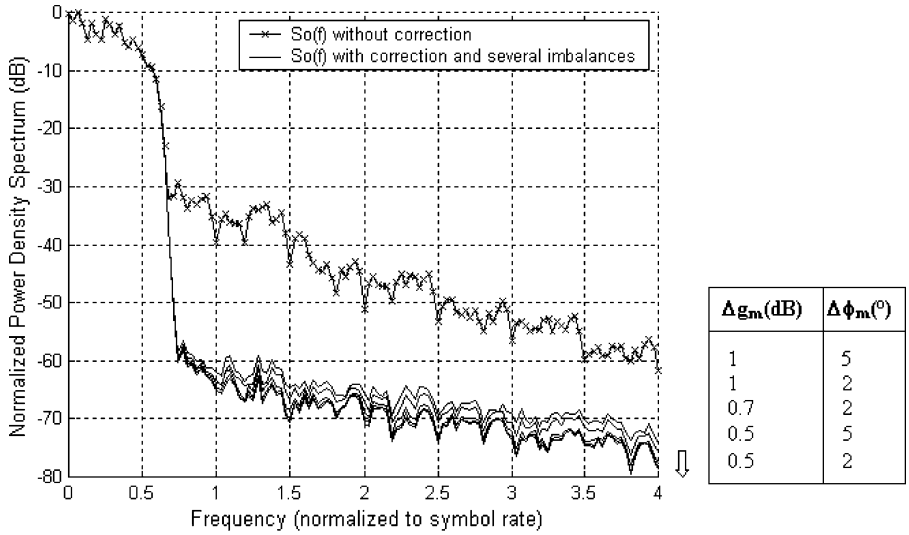

Fig. 8. Normalized power density spectrum of simulated input $S(f)$ and output $S_o(f)$ with several gain and phase imbalances in the quadrature modulator.

C. Method Viability

According to the presented simulations, the method performs well even with imbalances in the quadrature modulator and demodulator. In this section, we discuss the practical feasibility of the method.

Digital blocks of the design (such as SCS) and the calculation to update the adaptive coefficients K_1 and K_2 can be implemented in a powerful digital signal processor (DSP) device. Maximum optimization of the implementation of these algorithms is carried out approaching some DSP features, such as speed or special instructions for signal processing. The algorithms must be researched in order to decrease the number of instructions to reduce the computational load and introduce minimum delay in the system. The sampling rate in the DSP must be high enough to accommodate the feedback signal, which has much greater bandwidth than the desired signal. All previous presented results have been carried out with a sampling rate of 2.304 MHz, which is 128 times the TETRA symbol rate. A sampling rate too high supposes that all digital blocks in the DSP, mainly the signal component separator, must run at a much higher rate than without a correction method, and the ADC and DACs must be much faster. Some previous studies about the sampling rate in a LINC transmitter can be observed in [26]. Thus, research of the minimum necessary sampling rate in the proposed architecture to meet TETRA requirements regarding the ACI has been performed. Fig. 13 determines at least a sampling rate 64 times higher than the TETRA symbol rate, that is, 1.152 MHz.

We have also analyzed whether the value range of adaptive coefficients is suitable for implementation in a DSP. Fig. 14 shows this value range and its suitability. The simulations have been carried out with commercial imbalance values in I/Q modulator and demodulator.

Another important effect can be the quantization in the SCS block. The design is carried out according to the requirements described in [8], that determinate the minimum word length required for the SCS block and DACs. The signal component separator is implemented in a fixed-point DSP of a finite word length (16 bits). According to [8], this word length is suitable enough to achieve -60 dBc out-of-band emission (in the first

TABLE I
IMBALANCE VALUES IN BOTH QUADRATURE MODULATORS AND THE DEMODULATOR AND THE RESULTING ACI MEASUREMENT

I/Q Modulator in path 1		I/Q Modulator in path 2		I/Q Demodulator		ACI
Gain error	Phase error	Gain error	Phase error	Gain error	Phase error	
0.5 dB	5°	0.5 dB	5°	0.6 dB	5°	-62.86 dBc
0.5 dB	5°	0.2 dB	2°	0.6 dB	5°	-61.65 dBc
0.2 dB	2°	-0.2 dB	-2°	0.6 dB	5°	-61.8 dBc
0.2 dB	2°	-0.2 dB	-2°	0.45 dB	1.3°	-62.49 dBc

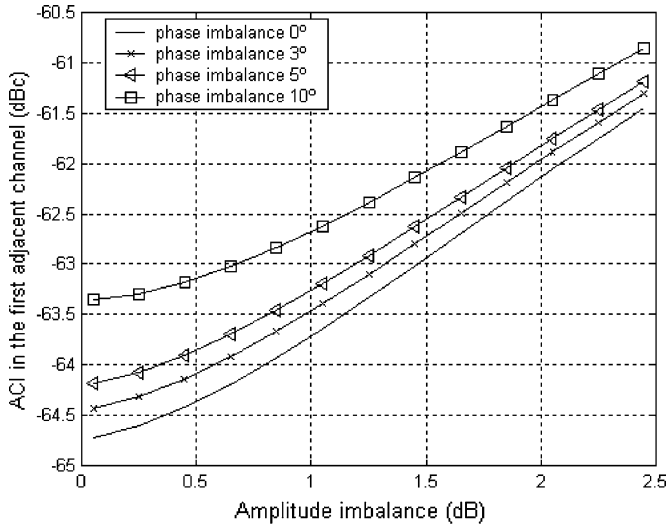

Fig. 9. Effect in this architecture of unbalanced modulators in the first ACI measurement.

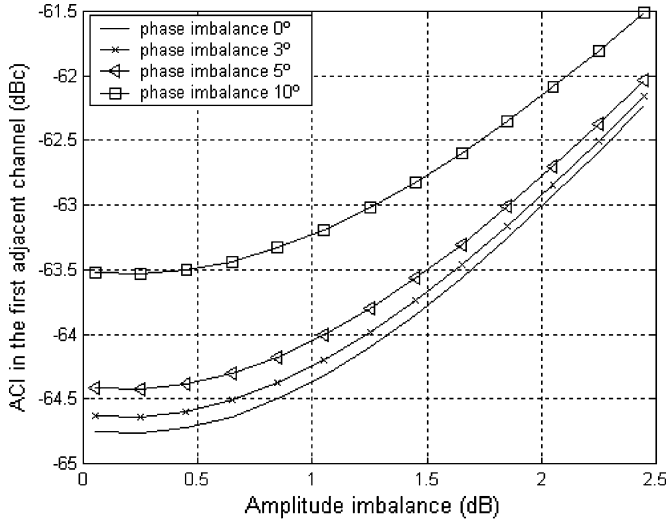

Fig. 10. Effect in this architecture of an unbalanced quadrature downconverter in the first ACI measurement.

adjacent channel). In the feedback branch, the effect of number of quantization bits for the ADC can be also analyzed. The quantization error of the ADC degrades the measurement accuracy and the algorithm convergence. Fig. 15 determines at least nine quantization bits for the ADC in order to meet the TETRA specifications regarding to interference in the first adjacent channel. The quantization effect will not be a problem in a real design with a right choice of DACs and the ADC in the current wide range of commercial devices (e.g. 12, 14, or 16 bits).

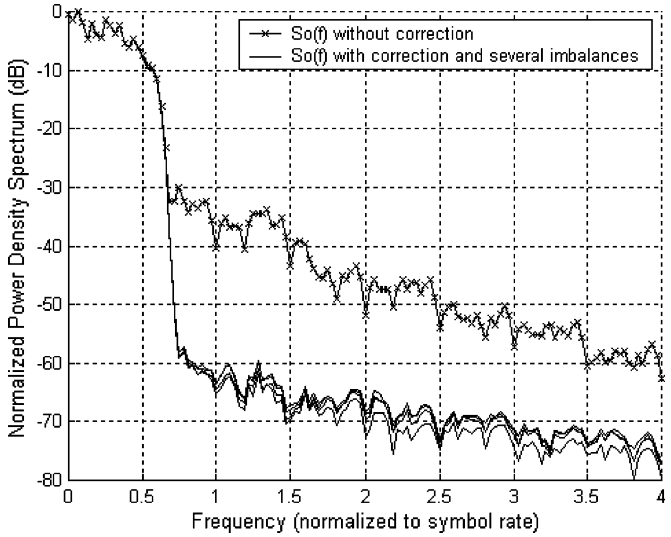

Fig. 11. Normalized power density spectrum of simulated input $S(f)$ and output $S_o(f)$ with several gain and phase imbalances in the quadrature modulator and demodulator.

Another ideal situation that has been assumed in the previous simulations corresponds to the nonzero loop delay. The reference signal $r(t)$ is a delayed and attenuated version of amplifier output $s_o(t)$. A temporal delay term τ is introduced in the reference branch to simulate this loop delay

$$r(t) = \frac{s_o(t-\tau)}{G_L}. \tag{24}$$

The delay must be compensated for the adaptive algorithm to correctly compare $s_n(t)$ to $r_n(t)$. The same DSP device generates signals $s_n(t)$ and $r_n(t)$, where $s_n(t)$ are obtained from the source signal $s(t)$ and $r_n(t)$ from the feedback signal $r(t)$. Thus, the delay compensation can be easily obtained by comparing the samples with the calculated loop delay. Therefore, the delay produced by the correction circuit has to be estimated before introducing the adaptive algorithm. A rough estimation can be carried out with the theoretical time delay of the components in the design or by applying some of the loop delay estimation techniques proposed by other authors [9], [10], [12], [16] or with some previous calibration. According to the simulation, the adaptive method runs correctly if the error in the delay estimation is less than 1 μs. Fig. 16 shows the error on the delay estimation influence in the ACI measurement. So, accurate delay matching is important to improve the performance of this method, but it is not a limitation when implementing it in a real system.

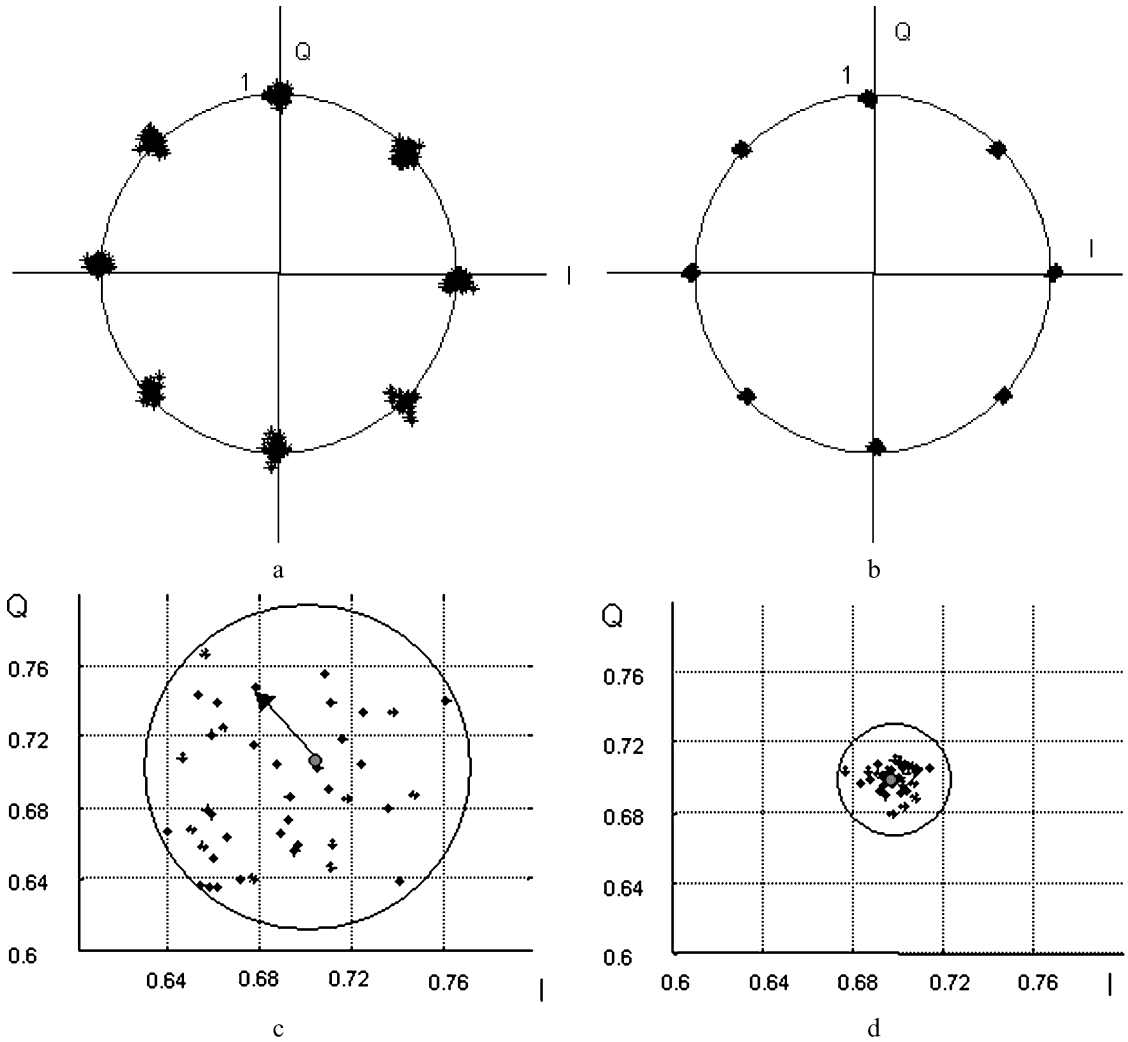

Fig. 12. Received signal constellation diagram without and with the correction method: (a) without the correction method, (b) with the correction method, (c) without the correction method, and (d) with the correction method.

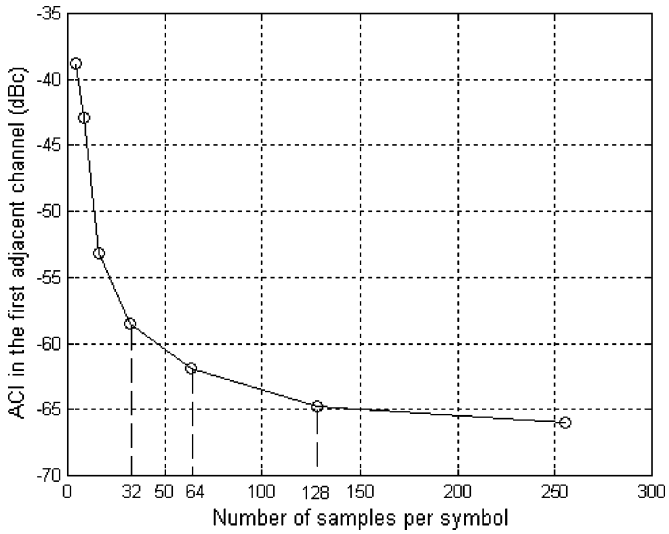

Fig. 13. Evolution of the ACI in the first adjacent channel (25 KHz) versus the number of samples per symbol.

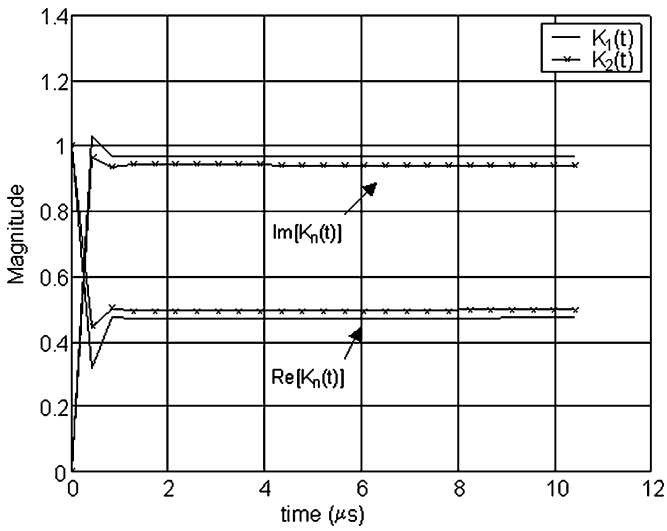

Fig. 14. Range of adaptive coefficients values K_1 and K_2.

V. Conclusion

A novel method to correct gain and phase imbalances in LINC transmitters has been described. Using a simulation, we have shown that it is possible to reduce the ACI to meet the restrictive specifications of the TETRA digital communication system. The system converges quickly toward very low interference levels in adjacent channels. As a result of its adaptive

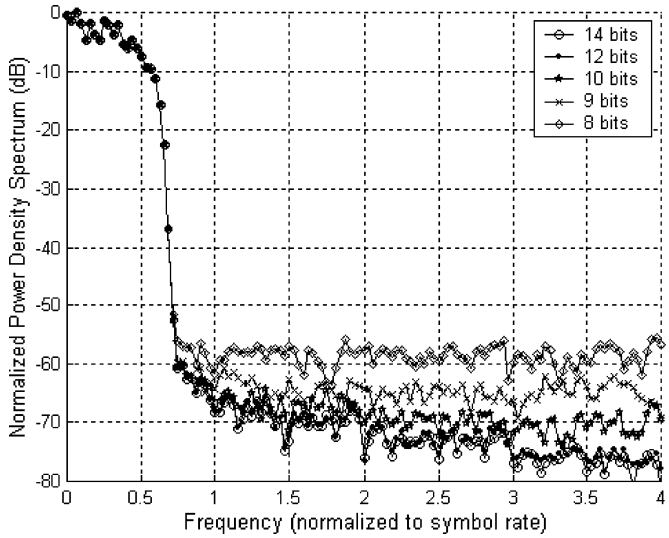

Fig. 15. Simulated $S_o(f)$ with 8, 9, 10, 12, and 14 quantization bits for the ADC in the feedback branch.

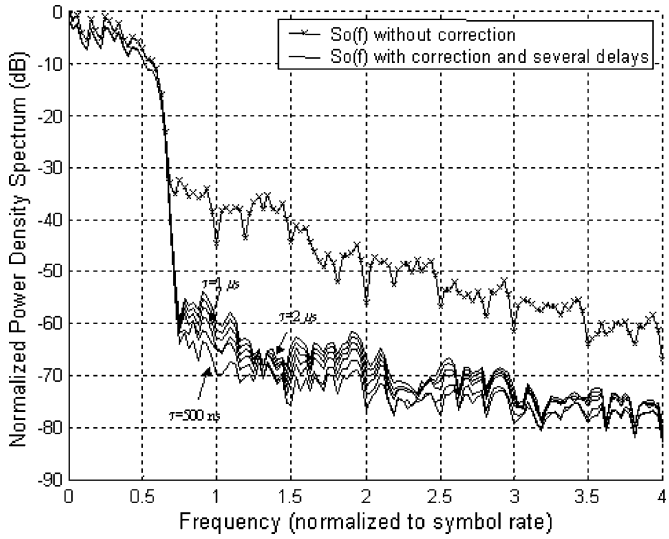

Fig. 16. Simulated $S_o(f)$ with several errors in the delay estimation.

technique, this method can track the input signal variations and possible changes due to variations in operating conditions. According to the simulation, the adaptive coefficient quickly reaches its optimal value, and the loop delay is not a problem if it is previously correctly estimated. Therefore, this method could be implemented in a real system by means a suitably powerful DSP device.

REFERENCES

[1] F. J. Casadevall and A. Valdovinos, "Performance analysis of QAM modulations applied to the LINC transmitter," *IEEE Trans. Veh. Technol.*, vol. 42, pp. 399–406, Nov. 1993.

[2] F. J. Casadevall and J. J. Olmos, "On the behavior of the LINC transmitter," in *Proc. 40th IEEE Veh. Tech. Conf.*, Orlando, FL, May 6–9, 1990, pp. 29–34.

[3] S. Tomisato, K. Chiba, and K. Murota, "Phase error free LINC modulator," *Electron. Lett.*, vol. 25, no. 9, pp. 576–577, Apr. 27, 1989.

[4] L. Sudström, "Automatic adjustment of gain and phase imbalances in LINC transmitters," *Electron. Lett.*, vol. 31, no. 3, pp. 155–156, Feb. 1995.

[5] S. Ampem-Darko and H. S. Al-Raweshidy, "Gain/phase imbalance cancellation technique in LINC transmitters," *Electron. Lett.*, vol. 34, no. 22, pp. 2093–2094, Oct. 1998.

[6] X. Zhang and L. E. Larson, "Gain and phase error-free LINC transmitter," *IEEE Trans. Veh. Technol.*, vol. 49, pp. 1986–1994, Sep. 2000.

[7] X. Zhang, L. E. Larson, P. M. Asbeck, and P. Nanawa, "Gain/phase imbalance-minimization techniques for LINC transmitters," *IEEE Trans. Microwave Theory Tech.*, vol. 49, pp. 2507–2516, Dec. 2001.

[8] L. Sundström, "The effect of quantization in a digital signal component separator for LINC transmitters," *IEEE Trans. Veh. Technol.*, vol. 45, pp. 346–352, May 1996.

[9] Y. Nagata, "Linear amplification technique for digital mobile communications," in *Proc. 39th IEEE Veh. Conf.*, May 1989, pp. 159–164.

[10] A. S. Wright and W. G. Durtler, "Experimental performance of and adaptive digital linearized power amplifier," *IEEE Trans. Veh. Technol.*, vol. 43, pp. 323–332, May 1994.

[11] S. A. Hetzel, A. Bateman, and J. P. McGeehan, "LINC transmitter," *Electron. Lett.*, vol. 27, no. 10, pp. 844–846, May 1991.

[12] J. de Mingo and A. Valdovinos, "Performance of a new digital baseband predistorter using calibration memory," *IEEE Trans. Veh. Technol.*, vol. 50, pp. 1169–1176, Jul. 2001.

[13] J. K. Cavers, "The effect of quadrature modulator and demodulator errors on adaptive digital predistorters for amplifier linearization," *IEEE Trans. Veh. Technol.*, vol. 46, pp. 456–466, May 1997.

[14] L. Sundström, "Spectral sensitivity of LINC transmitters to quadrature modulator misalignments," *IEEE Trans. Veh. Technol.*, vol. 49, pp. 1474–1487, Jul. 2000.

[15] P. B. Kenington, *High-Linearity RF Amplifier Design*. Reading, MA: Artech House, 2000.

[16] J. K. Cavers, "New methods for adaptation of quadrature modulators and demodulator in amplifier linearization circuits," *IEEE Trans. Veh. Technol.*, vol. 46, pp. 707–716, Aug. 1997.

[17] M. Faulkner and M. Johansson, "Adaptive linearization using predistortion. Experimental results," *IEEE Trans. Veh. Technol.*, vol. 43, pp. 323–332, May 1994.

[18] S. A. Maas, "Volterra analysis of spectral regrowth," *IEEE Microwave Guided Wave Lett.*, vol. 7, pp. 192–193, Jul. 1997.

[19] B. Stengel and W. R. Eisenstadt, "LINC power amplifier combiner method efficiency optimization," *IEEE Trans. Veh. Technol.*, vol. 49, pp. 229–234, Jan. 2000.

[20] C. P. Conradi, R. H. Johnston, and J. G. McRory, "Evaluation of a lossless combiner in a LINC transmitter," in *IEEE Can. Conf. Electrical Computer Engineering*, vol. 1, May 1999, pp. 105–110.

[21] L. Sündstrom and M. Johansson, "Effect of modulation scheme on LINC transmitter power efficiency," *Electron. Lett.*, vol. 30, no. 20, pp. 1643–1645, Sep. 1994.

[22] F. H. Raab, "Efficiency of outphasing RF power-amplifier systems," *IEEE Trans. Commun.*, vol. COM-33, pp. 1094–1099, Oct. 1985.

[23] B. Shi and L. Sündstrom, "Investigation of highly efficient LINC amplifier topology," in *IEEE Vehicular Technology Conf. Fall 2001*, vol. 2, Oct. 2001, pp. 1215–1219.

[24] G. T. Zhou and S. Kenney, "Predicting spectral regrowth of nonlinear power amplifiers," *IEEE Trans. Commun.*, vol. 50, pp. 718–722, May 2002.

[25] S. J. Grant, "A DSP controlled adaptive feedforward power amplifier linearizer," M.A.Sc. thesis, School of Engineering Science, Simon Fraser Univ., Jul. 1996.

[26] L. Sündstrom, "Effects of reconstruction filters and sampling rate for a digital signal component separator on LINC transmitter performance," *Electron. Lett.*, vol. 31, no. 14, pp. 1124–1125, Jul. 1995.

Paloma García was born in Zaragoza, Spain, in 1972. She received the Engineer of Telecommunications degree from the University of Zaragoza in 1996.

In 1995, she was with TELTRONIC SAU, where she worked in the Research and Development Department, involved in the design of radio communication systems (mobile equipment and base station) until 2002. From 1997 to 2001, she collaborated in several projects with the Communication Technologies Group of the Electronics Engineering and Communications Department, University of Zaragoza. In 2002, she joined the Centro Politécnico Superior, University of Zaragoza, where she is an Assistant Professor. She is also involved as a Researcher with the Aragon Institute of Engineering Research (I3A). Her research interests are in the area of linearization techniques of power amplifiers, and signal-processing techniques for radio communication systems.

Jesús de Mingo (M'98) was born in Barcelona, Spain, in 1965. He received the Ingeniero de Telecomunicación degree from the Universidad Politécnica de Cataluña, Barcelona, in 1991 and the Doctor Ingeniero de Telecomunicación degree from the Universidad de Zaragoza, Zaragoza, Spain, in 1997.

In 1991, he joined the Antenas Microondas y Radar group of the Departamento de Teoría de la Señal y Comunicaciones until 1992. In 1992, he was with MIER COMUNICACIONES S.A., where he worked in solid-state power amplifier design. In 1993, he became an Assistant Professor and in 2001 an Associate Professor in the Departamento de Ingeniería Electrínica y Comunicaciones, Universidad de Zaragoza. He is a member of the Aragon Institute of Engineering Research (I3A). His research interests are in the area of linearization techniques of power amplifiers, power amplifier design, and mobile antenna systems.

Antonio Valdovinos was born in Barbastro, Spain, in 1966. He received the Engineer of Telecommunications and Ph.D. degrees from the Universitat Politècnica de Catalunya (UPC), Spain, in 1990 and 1994, respectively.

In 1991 he joined, under a research grant, the Signal Theory and Communications Department, UPC, where he was an Assistant Professor. In 1995, he joined the Centro Politécnico Superior, Universidad de Zaragoza, Spain, where he became an Associate Professor in 1996 and a full Professor in 2003. He is a member of the Aragon Institute of Engineering Research (I3A). At present his research interest lies in the area of wireless communications with special emphasis on packet radio networks, wireless access protocols, radio resources management, and QoS.

Alfonso Ortega was born in Teruel, Spain, in 1976. He received the M.Sc. degree in telecommunication engineering from the University of Zaragoza, Zaragoza, Spain, in 2000.

In 1999 he joined, under a research grant, the Communications Technologies Group, University of Zaragoza, where he has been an Assistant Professor since 2001. He is also a Researcher with the Aragon Institute of Engineering Research (I3A). At present his research interest lies in the field of adaptive signal processing applied to radio communication systems and speech technologies.